

## Stability of the Fe electronic structure through temperature-, doping-, and pressure-induced transitions in the BaFe<sub>2</sub>As<sub>2</sub> superconductors

V. Balédent,<sup>1</sup> F. Rullier-Albenque,<sup>2</sup> D. Colson,<sup>2</sup> G. Monaco,<sup>3</sup> and J.-P. Rueff<sup>1,4,\*</sup>

<sup>1</sup>Synchrotron SOLEIL, Saint-Aubin, Boîte Postale 48, 91192 Gif-sur-Yvette Cedex, France

<sup>2</sup>SPEC CEA l'Orme les Merisiers, 91191 Gif-sur-Yvette Cedex, France

<sup>3</sup>ESRF, 6 Rue Jules Horowitz, Boîte Postale 220, 38043 Grenoble Cedex, France

<sup>4</sup>Laboratoire de Chimie Physique–Matière et Rayonnement, CNRS-UMR 7614, UPMC, 75005 Paris, France

(Received 8 October 2012; revised manuscript received 4 December 2012; published 17 December 2012)

We report on a survey of Fe electronic properties in the temperature-pressure phase diagram of the Co-doped pnictides BaFe<sub>2</sub>As<sub>2</sub> superconductors by hard x-ray absorption spectroscopy at the Fe *K* edge in the high-resolution, partial fluorescence yield mode. The absorption spectra are found remarkably stable through the temperature-induced phase transitions while pressure leads to slight energy shift of the main edge but not of the pre-edge. The latter effect is ascribed to the lattice compression and band widening effects under pressure as confirmed by multiple scattering simulations. Our results suggest that from the Fe electronic structure point of view, doping and pressure are equivalent ways to destabilize the magnetic phase to the advantage of superconductivity.

DOI: [10.1103/PhysRevB.86.235123](https://doi.org/10.1103/PhysRevB.86.235123)

PACS number(s): 74.70.Xa, 74.25.Jb, 78.70.Dm

A common feature of most unconventional superconducting materials is the existence of a magnetically ordered phase in their phase diagram.<sup>1,2</sup> The magnetic parent compound is usually considered from a formal point of view as the seminal seed from which the superconducting phases are derived. This applies, for instance, to the cuprates family, where superconductivity (SC) emerges from the magnetic phase either by doping or chemical substitution. In heavy fermions (HF), on the other hand,<sup>3,4</sup> SC appears under pressure within or and at the border of the magnetic phase. The Fe-based pnictides, the newly discovered family of superconductors, interestingly combines both aspects, as SC can be found either through pressure or doping changes.<sup>5,6</sup> This last class of superconductors has attracted a great deal of attention because of its similarity to the cuprates, its high critical temperature ( $\approx 40$  K) (Ref. 7), and the surprising presence of magnetic *3d* ions. The pnictides comprise in fact a wide variety of materials of different structures and chemical compositions, but all presenting a similar phase diagram. The relevant phases for this study are illustrated in Fig. 1(a) for Ba(Fe<sub>1-x</sub>Co<sub>x</sub>)<sub>2</sub>As<sub>2</sub>, one of the most studied families of pnictides. The undoped parent compound shows a spin density wave (SDW) magnetic order below  $T_{SDW}$  ( $\sim 138$  K). The transition to the SDW phase goes together with a tetragonal-orthorhombic transition.<sup>8</sup> Upon substituting K onto Ba or Co, Ni, Rh, and Pd onto the Fe sites,<sup>9-12</sup>  $T_{SDW}$  vanishes and superconductivity emerges. Under pressure, BaFe<sub>2</sub>As<sub>2</sub> becomes a superconductor, with  $T_c$  reaching 28 K at the optimal pressure of 5.5 GPa, as shown Fig. 1(b). Alternatively, an isovalent substitution of Fe by Ru also enables superconductivity.<sup>13</sup>

The ambivalent pressure or doping pathways to the SC phase, starting from the magnetic phase, raise the question of the exact role played by the two parameters and their equivalency. A recent structural study in Ba<sub>1-x</sub>K<sub>x</sub>Fe<sub>2</sub>As<sub>2</sub> reveals that pressure and doping affect similarly the Fe-Fe atomic distance and the Fe-As-Fe bond angle, suggesting that both control parameters operate in a similar fashion.<sup>14</sup> Such a simple picture, however, does not apply to the Co-doped family, which has spawned contradictory results. Co

substitution in Ba(Fe<sub>1-x</sub>Co<sub>x</sub>)<sub>2</sub>As<sub>2</sub>, for instance, was shown to leave the Fe electronic occupation at 300 K unchanged.<sup>15</sup> This seemingly indicates that the additional charge is localized on the Co sites rather than on the Fe sites, in agreement with recent theoretical predictions.<sup>16</sup> However, this mechanism contrasts with angle-resolved photoemission spectroscopy (ARPES) measurements<sup>17-20</sup> that report a gradual shift (about 20 meV) of the chemical potential upon doping, thus favoring a rigid band model in which Co donates its electron.

In this article, we aim to elucidate the roles of pressure and Co doping in the BaFe<sub>2</sub>As<sub>2</sub> family using high-resolution x-ray absorption spectroscopy (XAS) at Fe *K* edge as a probe of the Fe electronic states. A first, yet partial, answer has already been provided by Bittar *et al.*<sup>15</sup> The authors have studied the influence of Co substitution using XAS at the Fe *K* edge, but they could not detect any spectral changes up to  $x = 0.19$ . The measurements, however, were carried out at 300 K with moderate resolution, and they do not rule out possible changes through the SDW or SC transitions. Indeed, the Fe electrons are sensitive to their local environment via crystal-field strength, hybridization, and exchange interactions with neighboring atoms. Both SDW and SC transitions are expected to modify these interactions. In contrast in this study, the Fe valence is monitored by resolution-enhanced XAS through doping, pressure, and temperature transitions, spanning a wide region of the phase diagram [see the circles in Figs. 1(a) and 1(b)]. The results evidence the remarkable stability of the Fe electronic states throughout the pnictides phase diagram, further adding to their peculiar properties.

Single crystals of Ba(Fe<sub>1-x</sub>Co<sub>x</sub>)<sub>2</sub>As<sub>2</sub> were grown using the self-flux method.<sup>21</sup> Starting reagents of high-purity Ba, FeAs, and CoAs were mixed in the molar ratio 1 : (4 -  $x$ ) :  $x$ , loaded in alumina crucibles, and then sealed in evacuated quartz tubes. For each doping level, a chemical analysis was performed by an electron probe on several crystals yielding the Co content within 0.5% absolute accuracy. XAS at the Fe *K* edge was performed at the ID16 beamline at the European Synchrotron Radiation Facility (ESRF) in the partial fluorescence yield (PFY), high-resolution mode. Toward that end, the Fe *K* $\alpha$

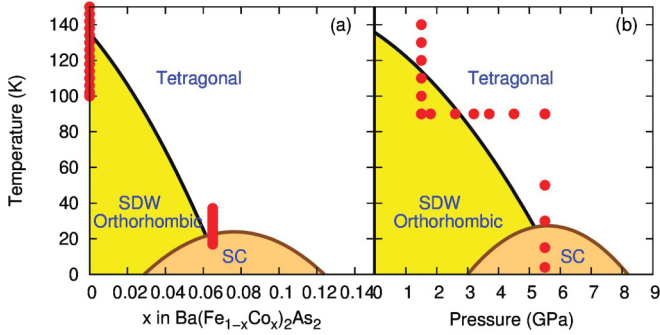


FIG. 1. (Color online) Temperature-doping (a) and temperature-pressure (b) phase diagram of  $\text{Ba}(\text{Fe}_{1-x}\text{Co}_x)_2\text{As}_2$ . Filled circles indicate the points where spectroscopic measurements have been performed.

( $2p \rightarrow 1s$  transition) emission line intensity was recorded as a function of the incident energy. The detection setup includes a 1 m spherically bent Ge(440) analyzer and an avalanche photon diode detector laid out in the Rowland circle geometry. In the PFY configuration, the  $1s$  core-hole lifetime broadening effect is partly removed, being superseded by the sharper  $2p$  width left out in the final state, thus providing XAS spectra with improved intrinsic resolution. For high-pressure, low-temperature measurements, the samples (60  $\mu\text{m}$  wide, 20  $\mu\text{m}$  thick) were loaded in a membrane-driven diamond anvil cell (DAC) with silicon oil as a pressure transmitting medium; the DAC was then mounted in a closed-loop He cryostat. The pressure inside the DAC was estimated using the ruby fluorescence technique yielding a precision below 0.5 GPa, taking into account the temperature dependence.<sup>22,23</sup> All data were corrected from self-absorption.

We first focus on the parent, undoped compound at ambient pressure to investigate the SDW transition. The normalized Fe  $K$ -edge XAS spectra are shown in Fig. 2(a) for temperature ranging from 100 to 160 K with a step of 4 K. The spectra are composed of an intense white-line peaking at 7122 keV related to  $1s \rightarrow 4p$  dipolar transitions, preceded by a weaker pre-edge feature around 7110.5 eV. Because Fe sits in a noncentrosymmetric tetrahedral site, the latter structure is not of pure quadrupolar  $3d$  character but shows an admixture of  $p$  and  $d$  states.<sup>24</sup> The spectral differences with respect to high temperature are also shown. No change of line shape nor energy shift can be observed across the SDW transition, revealing that the Fe site does not undergo any modification of its local electronic or structural properties. Remarkably, a similar behavior is found in the optimally doped sample  $\text{Ba}(\text{Fe}_{0.935}\text{Co}_{0.065})_2\text{As}_2$  at low temperatures [cf. Fig. 2(b)]. Overall, these results primarily suggest that the structural transition accompanying the SDW ordering entails no drastic change of the Fe electronic properties and/or crystal field symmetry. Combining these results with the reported Fe valence stability under doping at ambient temperature,<sup>15</sup> we can first conclude that there is a remarkable stability of the Fe electronic states upon doping or temperature changes.

Pressure, on the other hand, usually has a stronger effect on the local electronic properties compared to temperature or doping, as it acts directly on the interatomic distance and hybridization. The investigation of the pressure-induced

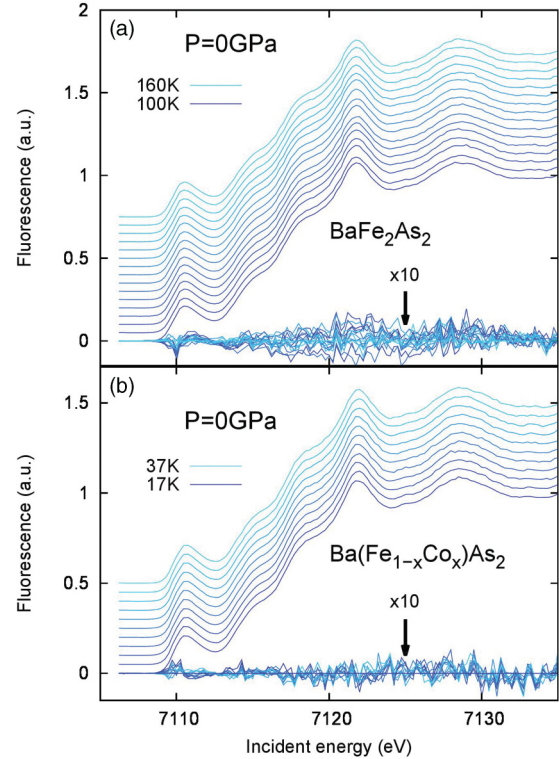


FIG. 2. (Color online) Fe  $K$ -edge absorption spectra in the parent  $\text{BaFe}_2\text{As}_2$  (a) and optimally doped compounds  $\text{Ba}(\text{Fe}_{1-x}\text{Co}_x)_2\text{As}_2$  ( $x = 0.065$ ) (b) as a function of temperature at ambient pressure. The two datasets correspond to the transitions through the SDW ( $T_{\text{SDW}} \approx 130$  K) for  $\text{BaFe}_2\text{As}_2$  (a) and superconducting phase boundaries ( $T_c \approx 27$  K) as indicated in Fig. 1(a). The spectral differences with respect to the highest temperature are shown in each panel below the absorption spectra, after multiplication by a factor 10.

transition also brings us closer to the seminal question of the equivalence between pressure-induced and doping-induced transitions. To that aim, we first applied a pressure of 1.5 GPa, where  $T_{\text{SDW}}$  is reduced to  $\approx 110$  K,<sup>25</sup> and then we changed temperature at constant pressure from 90 to 140 K with a 10 K step. Second, pressure was increased to 5.5 GPa with  $T_c$  approaching its maximum value of 27 K in order to study the superconducting transition. The spectra for both temperature-induced SDW (1.5 GPa) and superconducting transitions (5.5 GPa) are reported in Figs. 3(a) and 3(b), respectively. In spite of a significant decrease in count rate due to the absorption by the diamond anvils and the smaller sample size, no alteration of the spectra can be detected when varying temperature at 1.5 and 5.5 GPa. This is further confirmed by inspection of the difference spectra that show barely any changes with temperature.

At this point, it is important to discuss the sensitivity of XAS to doping change. Cuprates can be used in the first place as model systems. According to Ref. 26,  $\text{La}_{2-x}\text{Sr}_x\text{CuO}_4$  experiences a shift of chemical potential of 25 meV for  $x = 0.055$  while the corresponding Cu  $K$ -edge spectra show a strong and visible effect in both shape and energy position.<sup>27</sup> A chemical shift of similar amplitude is estimated in the optimally doped  $\text{Ba}(\text{Fe}_{0.935}\text{Co}_{0.065})_2\text{As}_2$  compound with respect to the undoped compound.<sup>20</sup> Notice that in more ionic compounds, such as

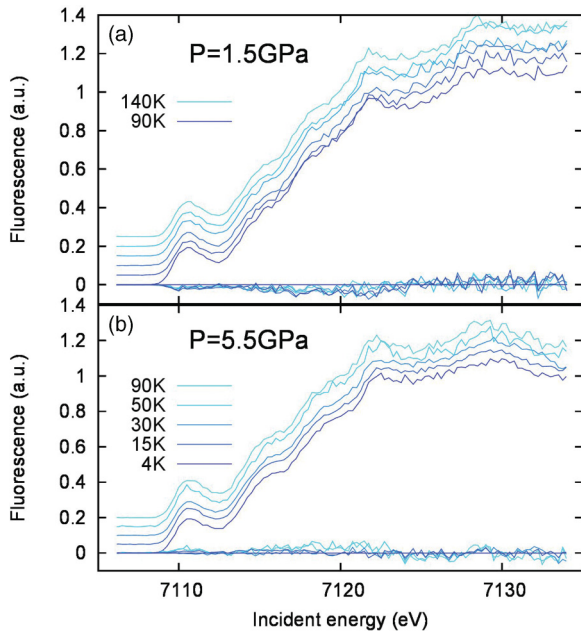


FIG. 3. (Color online) Fe  $K$ -edge absorption spectra for  $\text{BaFe}_2\text{As}_2$  as a function of temperature at constant pressure, respectively, of 1.5 GPa (a) and 5.5 GPa (b). These two series of data correspond to the temperature evolution through the SDW [ $T_{\text{SDW}} \approx 110$  K (Ref. 25)] at 1.5 GPa (a) and the superconducting transition at 5.5 GPa ( $T_c \approx 27$  K) as indicated in Fig. 1(b). Spectral difference with respect to the lowest pressure data is shown below the spectra.

manganites<sup>28</sup> or Fe minerals,<sup>29</sup> the Mn  $K$  edge is reported to shift by several eV when the oxidation state is changed by unity. This yields a sensitivity of a few percent of electron variation, considering the experimental resolution. All in all, we expect that electronic changes equivalent to that of a few percent doping should be visible in the Fe  $K$  edge of pnictides, which is not the case.

The last step to complete our survey of the Fe electronic properties is the pressure dependence at constant temperature. The corresponding spectra measured at  $T = 90$  K are reported in Fig. 4(a). We observe slight modifications of the spectra with pressure, but these mostly affect the high-energy region of  $p$  character that progressively shifts toward high energy; in contrast, the pre-edge region sensitive to the  $d$  states is barely modified except for a noticeable broadening effect [cf. the lines in Fig. 4(a)]. The spectral changes are highlighted in Fig. 4(b) for the two extreme pressure points. The overall behavior under pressure is ascribed to the regular shortening of the interatomic distance under high pressure and band widening effects. To confirm this interpretation, we performed numerical simulation of the Fe  $K$  edge using the FEFF8 code.<sup>30</sup> As starting parameters, we used the crystal structures of Ref. 31, respectively orthorhombic (space group  $Fm\bar{3}m$ ) at 1.5 GPa and tetragonal (space group  $I4/m\bar{3}m$ ) at 5.5 GPa. The atomic potential was calculated self-consistently using a cluster of up to 32 atoms within a radius of 5.5 Å in the muffin-tin approximation. Both dipolar and quadrupolar transitions were taken into account. The full multiple scattering XAS calculations converge for a cluster of 154 atoms within

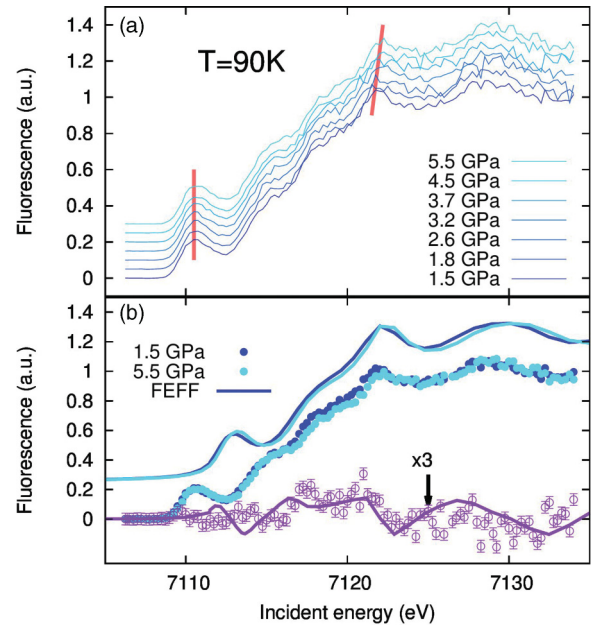


FIG. 4. (Color online) (a) Fe  $K$ -edge absorption spectra for  $\text{BaFe}_2\text{As}_2$  as a function of pressure at constant temperature  $T = 90$  K through the SDW pressure transition ( $P_{\text{SDW}} \approx 3$  GPa), as indicated in Fig. 1(b); the thick lines indicate the energy position of specific spectral features in the pre-edge and post-edge region, highlighting their differing behaviors. (b) Experimental spectra at low (1.5 GPa) and optimal pressure (5.5 GPa) and FEFF8 CALCULATED SPECTRA AND THEIR SPECTRAL DIFFERENCES (SEE TEXT FOR DETAILS).

the radius of 9 Å. The results for the two structures are represented in Fig. 4(b) together with experimental data. The high-energy features are well reproduced by the calculations but not the low-energy part, especially in the pre-edge region. This discrepancy, already reported in Ref. 15, is likely due to a poor description of the correlated  $d$  states. Nevertheless, the calculations succeed in reproducing the main spectral changes with pressure (see the difference spectrum) corroborating the structural origin of the energy shift.

In conclusion, we find a remarkable stability of Fe electronic properties through temperature-, doping-, or pressure-induced transitions in the  $\text{Ba}(\text{Fe}_{1-x}\text{Co}_x)_2\text{As}_2$  family. Thus Co doping and pressure are two equivalent ways to cross the phase diagram from the point of view of the Fe bulk electronic structure. Unlike ARPES, which shows a clear dependence of the chemical potential with doping,<sup>20</sup> none of the control parameters investigated in this study has a definite impact on the Fe electronic states. This apparent contradiction can be tentatively ascribed to experimental limitations: ARPES is a very surface-sensitive probe compared to XAS and could perceive a different electronic structure. We propose another scenario, yet to be confirmed, that could reconcile both results. The Co doping could primarily affect the As electronic levels. In such a case, changes of the Fermi surface as observed by ARPES would come from a perturbation of the As density of states, while the Fe-projected electronic properties would remain unaffected.

\*Author to whom all correspondence should be addressed: rueff@synchrotron-soleil.fr

- <sup>1</sup>A. J. Leggett, *Nat. Phys.* **2**, 134 (2006).
- <sup>2</sup>J. Zhao, Q. Huang, C. de la Cruz, S. Li, J. W. Lynn, Y. Chen, M. A. Green, G. F. Chen, G. Li, Z. Li, J. L. Luo, N. L. Wang, and P. Dai, *Nat. Mater.* **7**, 953 (2008).
- <sup>3</sup>R. Movshovich, T. Graf, D. Mandrus, J. D. Thompson, J. L. Smith, and Z. Fisk, *Phys. Rev. B* **53**, 8241 (1996).
- <sup>4</sup>N. D. Mathur, F. M. Grosche, S. R. Julian, I. R. Walker, D. M. Freye, R. K. W. Haselwimmer, and G. G. Lonzarich, *Nature (London)* **394**, 39 (1998).
- <sup>5</sup>J. Paglione and R. L. Greene, *Nat. Phys.* **6**, 645 (2010).
- <sup>6</sup>I. Mazin, *Nature (London)* **464**, 183 (2010).
- <sup>7</sup>H. Takahashi, K. Igawa, K. Arii, Y. Kamihara, M. Hirano, and H. Hosono, *Nature (London)* **453**, 376 (2008).
- <sup>8</sup>M. Rotter, M. Tegel, D. Johrendt, I. Schellenberg, W. Hermes, and R. Pöttgen, *Phys. Rev. B* **78**, 020503 (2008).
- <sup>9</sup>M. Rotter, M. Tegel, and D. Johrendt, *Phys. Rev. Lett.* **101**, 107006 (2008).
- <sup>10</sup>A. S. Sefat, R. Jin, M. A. McGuire, B. C. Sales, D. J. Singh, and D. Mandrus, *Phys. Rev. Lett.* **101**, 117004 (2008).
- <sup>11</sup>L. J. Li, Y. K. Luo, Q. B. Wang, H. Chen, Z. Ren, Q. Tao, Y. K. Li, X. Lin, M. He, Z. W. Zhu, G. H. Cao, and Z. A. Xu, *New J. Phys.* **11**, 025008 (2009).
- <sup>12</sup>N. Ni, A. Thaler, A. Kracher, J. Q. Yan, S. L. Bud'ko, and P. C. Canfield, *Phys. Rev. B* **80**, 024511 (2009).
- <sup>13</sup>F. Rullier-Albenque, D. Colson, A. Forget, P. Thuéry, and S. Poissonnet, *Phys. Rev. B* **81**, 224503 (2010).
- <sup>14</sup>S. A. J. Kimber, A. Kreyssig, Y.-Z. Zhang, H. O. Jeschke, R. Valenti, F. Yokaichiya, E. Colombier, J. Yan, T. C. Hansen, T. Chatterji, R. J. McQueeney, P. C. Canfield, A. I. Goldman, and D. N. Argyriou, *Nat. Mater.* **8**, 471 (2009).
- <sup>15</sup>E. M. Bittar, C. Adriano, T. M. Garitezi, P. F. S. Rosa, L. Mendonça-Ferreira, F. Garcia, G. de M. Azevedo, P. G. Pagliuso, and E. Granado, *Phys. Rev. Lett.* **107**, 267402 (2011).
- <sup>16</sup>H. Wadati, I. Elfimov, and G. A. Sawatzky, *Phys. Rev. Lett.* **105**, 157004 (2010).
- <sup>17</sup>V. Brouet, M. Marsi, B. Mansart, A. Nicolaou, A. Taleb-Ibrahimi, P. Le Fèvre, F. Bertran, F. Rullier-Albenque, A. Forget, and D. Colson, *Phys. Rev. B* **80**, 165115 (2009).
- <sup>18</sup>S. Thirupathaiah, S. de Jong, R. Ovsyannikov, H. A. Dürr, A. Varykhalov, R. Follath, Y. Huang, R. Huisman, M. S. Golden, Y.-Z. Zhang, H. O. Jeschke, R. Valentí, A. Erb, A. Gloskovskii, and J. Fink, *Phys. Rev. B* **81**, 104512 (2010).
- <sup>19</sup>C. Liu, A. D. Palczewski, R. S. Dhaka, T. Kondo, R. M. Fernandes, E. D. Mun, H. Hodovanets, A. N. Thaler, J. Schmalian, S. L. Bud'ko, P. C. Canfield, and A. Kaminski, *Phys. Rev. B* **84**, 020509 (2011).
- <sup>20</sup>M. Neupane, P. Richard, Y.-M. Xu, K. Nakayama, T. Sato, T. Takahashi, A. V. Federov, G. Xu, X. Dai, Z. Fang, Z. Wang, G.-F. Chen, N.-L. Wang, H.-H. Wen, and H. Ding, *Phys. Rev. B* **83**, 094522 (2011).
- <sup>21</sup>F. Rullier-Albenque, D. Colson, A. Forget, and H. Alloul, *Phys. Rev. Lett.* **103**, 057001 (2009).
- <sup>22</sup>H. K. Mao, J. Xu, and P. M. Bell, *J. Geophys. Res.* **91**, 4673 (1986).
- <sup>23</sup>S. Rekhı, L. S. Dubrovinsky, and S. K. Saxena, *High Temp. High Press.* **31**, 299 (1999).
- <sup>24</sup>M.-A. Arrio, S. Rossano, C. Brouder, L. Galois, and G. Calas, *Europhys. Lett.* **51**, 454 (2000).
- <sup>25</sup>E. Colombier, S. L. Bud'ko, N. Ni, and P. C. Canfield, *Phys. Rev. B* **79**, 224518 (2009).
- <sup>26</sup>G. Rietveld, M. Glastra, and D. van der Marel, *Physica C* **241**, 257 (1995).
- <sup>27</sup>N. Kosugi, Y. Tokura, H. Takagi, and S. Uchida, *Phys. Rev. B* **41**, 131 (1990).
- <sup>28</sup>G. Subías, J. García, M. G. Proietti, and J. Blasco, *Phys. Rev. B* **56**, 8183 (1997).
- <sup>29</sup>M. Wilke, F. Farges, P.-E. Petit, G. E. Brown, and F. Martin, *Am. Mineral.* **86**, 714 (2001).
- <sup>30</sup>A. L. Ankudinov, B. Ravel, J. J. Rehr, and S. D. Conradson, *Phys. Rev. B* **58**, 7565 (1998).
- <sup>31</sup>E. Granado, L. Mendonça-Ferreira, F. Garcia, G. de M. Azevedo, G. Fabbri, E. M. Bittar, C. Adriano, T. M. Garitezi, P. F. S. Rosa, L. F. Bufaical, M. A. Avila, H. Terashita, and P. G. Pagliuso, *Phys. Rev. B* **83**, 184508 (2011).